

# The Wave Carpet: Development of a Submerged Pressure Differential Wave Energy Converter

Marcus Lehmann, Ryan Elandt, Mostafa Shakeri, & Reza Alam  
(University of California, Berkeley, USA)

## ABSTRACT

Inspired by the natural phenomenon of strong attenuation of oceanic surface waves by muddy seafloors, the Theoretical and Applied Fluid Dynamics Laboratory at the University of California, Berkeley, has recently investigated a mud-resembling synthetic compliant seabed carpet (so called Wave Carpet), composed of linear springs and generators, that can be used as an efficient wave energy conversion device. Wave Carpet has a theoretical efficiency of unity and a broad bandwidth of high performance. It is also omnidirectional, and since it sits under the water surface it is highly survivable against the high momentum of storm waves, while at the same time poses minimal danger to the sealife as well as minimal visual pollution. Here we present a basic analytical model, development and optimization of a scaled prototype for the wave tank test, and the experimental results and discussions. Experimental results positively endorse the wave carpet's capability to absorb and convert wave energy efficiently in different wave conditions. Wave Carpet is classified as a submerged pressure-differential wave energy converter.

## INTRODUCTION

One of the major challenges of the 21st centuries is to meet the constantly increasing global energy demand. Approximately 3 billion people live within 200 km of the world's coastlines, and while this number is expected to double by 2025 (mainly due to migration, see e.g. Creel, 2003), the resources provided by the adjacent oceans are hardly being used. For example, world's wave power potential alone is estimated to be 29,500 TWh/year, with the power density ranging from 50 to 125 kW/m at latitudes near 40 degrees (Mork &

Kabuth, 2010).

Despite this level of potential, ocean wave energy has not yet been commercialized. One main obstacle is the survivability in the harsh ocean environment and its associated costs. It is to be noted that while there are many lessons to be learned and many ideas that can be borrowed from the well-developed offshore industry, one major differentiating factor between ocean wave energy and offshore structures is that wave harvesting devices must be working at (or near) the resonance, whereas offshore structures work as far away as possible from the resonance. Environmental aspects, permitting and jurisdictional issues, extracting power from a low-frequency up-down motion (e.g. note the contrast with the wind power), polychromatic and multidirectional nature of oceanic waves, and complexity of the highly nonlinear and complex behavior of such waves are existing challenges that are yet to be addressed.

Ocean wave energy is sometimes compared with the wind industry some 25 years ago when there was neither a unique design, nor a universal agreement on its future path. Wind industry has converged to a single now-familiar design over the past quarter of a century and now is a major player in the renewable energy industry. Having learned from the evolution of wind power, wave power is expected to come into equal or more play in a much shorter time period.

Toward this goal, we have recently investigated a novel wave energy harvesting device which is inspired by the observation of strong wave attenuation by the seafloor mud (Alam, 2012a). It is known that muddy seafloors can extract significant energy from overpassing surface waves via engaging them in strong interaction processes (see Fig. 1). Gade (1958) reports a place in the gulf of Mexico known to locals as *mud hole* where due to the accretion of mud banks has turned



**Figure 1:** This amazing airborne photo shows how a small strip of muddy seabed (darker part of the sea from center to the right) can strongly attenuate surface waves. The photo shows a part of Cassino Beach (Brazil) that has a strip of very muddy seafloor on the right and a rigid seafloor on the left. Clearly wave breaking (i.e. white capping in the photo, a measure of wave energy) is much less on the muddy side (i.e. right-side of the photo), where most of the incident wave energy has been damped by the mud (Photo from Holland et al., 2009)

into, for the local fishermen, a safe haven against strong waves during storms. Within the mud hole the interaction of surface waves with the mud is very strong such that waves completely damped out within a few wavelengths (Elgar and Raubenheimer, 2008). Observations of strong wave damping due to the coupling with the bottom mud is not limited to the gulf, but almost anywhere with a very muddy seafloor (e.g. Silvester, 1974; Macpherson and Kurup, 1981; Sheremet and Stone, 2003).

Motivated by this natural phenomenon of strong attenuation of oceanic surface waves by muddy seafloors, we have recently investigated a mud-resembling synthetic compliant seabed carpet, composed of linear springs and generators (see fig. 2), that can be used as an efficient wave energy absorption device (Alam, 2012a,b; Lehmann et al., 2013). The idea, has several advantages over previously considered ideas:

1. The carpet of wave energy harvesting (or simply the Wave Carpet) can absorb the entire energy content of incident waves (narrow or broadband) hence has a theoretical efficiency of unity. This is more highlighted when compared with other ideas of harnessing ocean power. For instance “Oscillating Wave Surge Converters” have a theoretical efficiency of 50%<sup>1</sup>.
2. The Wave Carpet has a broad bandwidth of high-

<sup>1</sup>The 100% efficiency in the *absorption* is also expected to be achievable in practice since the natural counterpart, i.e. mud, can too completely damp energy of overpassing waves (see e.g. Gade, 1958; Silvester, 1974; Macpherson and Kurup, 1981; Sheremet and Stone, 2003). Note that the overall efficiency is absorption efficiency times the *conversion* efficiency.

performance. This property makes it more suited to realistic ocean environment where waves typically form a wide spectrum of different frequencies.

3. It is omni-directional, that is, it can absorb the energy of incoming waves that are coming from all different directions.
4. The Wave Carpet is completely under the water surface hence imposes minimal danger to boats and the sea life (i.e. no mammal entanglement), and also causes no visual pollution.
5. The carpet is survivable against high momentum of storm surges because the water column above it acts as a buffer. In fact Wave Carpet can perform even better under very energetic (e.g. stormy) sea conditions, when most existing wave energy devices are needed to shelter themselves by going into an idle mode,
6. The Wave Carpet idea and its variations may also be used to create localized safe havens for fishermen and sailors in open seas, or if implemented in large scales to protect shores and harbors against strong storm waves.

The Wave Carpet system (Fig. 2) is governed by a nonlinear and coupled set of equations that include the dynamics of gravity waves and the visco-elastic seabed. The linearized form of the set of governing equations admit a surface-mode and a bottom-mode eigen-solution. While damping of surface-mode waves is higher for longer waves, the damping of a bottom-mode wave is higher for shorter waves. Furthermore, computational investigation of nonlinear interactions of surface waves and the WEC have shown that the rate of energy extraction increases for steeper surface waves (Alam, 2012b).

The subject of this paper is to review theoretical description of the Wave Carpet and to present experimental investigation of the first model-based prototype (c.f. Lehmann et al., 2013, for a proof-of-concept experiment). This paper describes the constructional steps taken to transfer the carpet concept into a first working prototype and it presents the experimental results of the developed converter while operating under the influence of a variety of wave conditions.

In section II, the governing equations that describe the analytical model are provided. Section III describes the engineering design, the steps taken from the abstract mechanical model to the first working and revised prototype along with the constructional solution of the required components of the system. Section IV presents

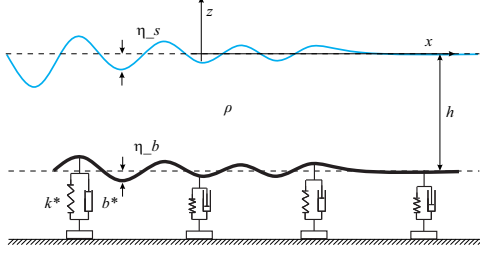


**Figure 2:** Schematic diagram of a viscoelastic carpet on the seafloor for extracting energy from surface gravity waves. The carpet is composed of linear springs with the stiffness coefficient  $k^*$  that provide the restoring force, and generators with damping coefficient  $b^*$  that extract energy. The distance between each module of the spring damper is assumed much smaller than the typical wavelength of the overpassing waves such that the assumption of continuously distributed spring-dampers is valid.

the conducted experiments and the results. The discussion in Section V emphasizes the advantages of this novel WEC and provides an outlook of the system. Finally, section VI summarizes the presented research.

## ANALYTICAL MODELING

Consider a homogeneous inviscid incompressible fluid with irrotational motion. The bottom at the mean depth  $z = -h$  is regarded viscoelastic (Fig. 2). The equations of the velocity potential  $\phi$  and the surface and bottom elevations  $\eta_s$  and  $\eta_b$  neglecting the surface tension read as:

$$\nabla^2 \phi = 0, \quad -h + \eta_b < z < \eta_s, \quad (1a)$$

$$\eta_{s,t} + \eta_{s,x} \phi_x = \phi_z, \quad z = \eta_s, \quad (1b)$$

$$\phi_t + \frac{1}{2}(\phi_x^2 + \phi_z^2) + g\eta_s = 0, \quad z = \eta_s, \quad (1c)$$

$$\eta_{b,t} + \eta_{b,x} \phi_x = \phi_z, \quad z = -h + \eta_b, \quad (1d)$$

$$\phi_t + \frac{1}{2}(\phi_x^2 + \phi_z^2) + g\eta_b + \frac{P_b}{\rho} = 0, \quad z = -h + \eta_b, \quad (1e)$$

$$b^* \eta_{b,t} + k^* \eta_b + P_b = 0, \quad z = -h + \eta_b \quad (1f)$$

with the gravity acceleration  $g$ , the density of the fluid  $\rho$ , the pressure on the seabed  $P_b$ , the viscous damping  $b^*$  and the stiffness coefficient of the viscoelastic bottom per unit area  $k^*$ . The linearized form of governing

equations admits a propagating wave in the form of

$$\eta_s = a_s e^{i(kx - \omega t)}, \quad (2a)$$

$$\eta_b = a_b e^{i(kx - \omega t)}, \quad (2b)$$

$$\phi = (A e^{kz} + B e^{-kz}) e^{i(kx - \omega t)} \quad (2c)$$

where

$$a_b = a_s \cosh kh \left( 1 - \frac{gh \tanh kh}{\omega^2} \right), \quad (3)$$

$$A = -i a_s \frac{\omega^2 + gk}{2k\omega}, \quad B = i a_s \frac{\omega^2 - gk}{2k\omega},$$

with the surface amplitude  $a_s$  and the bottom amplitude  $a_b$ . Furthermore, the dispersion relation reads in dimensionless form

$$\gamma \Omega^4 \tanh(\mu) + i \mu \gamma \zeta \Omega^3 - \mu \Omega^2 - i \mu^2 \gamma \zeta \Omega \tanh(\mu) + \mu^2 (1 - \gamma) \tanh(\mu) = 0 \quad (4)$$

The dimensionless variables are

$$\Omega = \omega \sqrt{h/g}, \quad \zeta = \frac{b^*}{\rho \sqrt{gh}}, \quad \gamma = \frac{\rho g}{k^*}, \quad \text{and } \mu = kh \quad (5)$$

with the dimensionless frequency  $\Omega$ , the dimensionless damping ratio  $\zeta$ , the dimensionless restoring force  $\gamma$  and the shallowness  $\mu$ .

The average energy stored in one piston damper over one period of time is

$$\overline{E_p} = \int_0^T F_p \cdot v_p dt = \int_0^T b \omega^2 a_b^2 \cos^2(\omega t) dt = \frac{2\pi^2 b a_b^2}{T} \quad (6)$$

with  $v_p = \omega a_b \cos(\omega t)$  where  $a_b$  is the amplitude of the bottom and  $b$  the damping coefficient of one generator. Here the damping coefficient is simplified as being constant.

The energy stored in the carpet per unit area for a undamped system is described as

$$E_{tot} = E_{kin} + E_{pot} = \frac{1}{2} \rho g a_s^2 D \quad (7)$$

with

$$E_{kin} = \frac{1}{2} \rho g a_s^2 \left\{ \frac{\sinh 2kh}{2} \left( \frac{\omega^2}{gk} + \frac{gk}{\omega^2} \right) - 2 \sinh^2 kh \right\} \quad (8)$$

$$E_{pot} = \frac{1}{4} \rho g (a_s^2 - a_b^2) + \frac{1}{4} k^* a_b^2 \quad (9)$$

and the dimensionless constant  $D$

$$D = \frac{\sinh 2kh}{2} \left( \frac{\omega^2}{gk} + \frac{gk}{\omega^2} \right) - 2 \sinh^2 kh + \frac{a_s^2 - a_b^2}{a_s^2} + \frac{k^* a_b^2}{2 \rho g a_s^2}. \quad (10)$$

Therefore

$$E_{tot} = \frac{1}{2} \rho g a_s^2 \left\{ \frac{\sinh 2kh}{2} \left( \frac{\omega^2}{gk} + \frac{gk}{\omega^2} \right) - 2 \sinh^2 (kh) + \rho g (a_s^2 - a_b^2) + k^* a_b^2 \right\} \quad (11)$$

The solution of 4 gains an imaginary part  $\omega = \omega_r + i\omega_i$  if damping is present. The dimensionless constant  $D$  is then written as  $D_d$

$$D_d = \frac{1}{2} \left( \frac{\sinh(2\mu)}{2} \left( \frac{\Omega_r r^2}{\mu} + \frac{\mu}{\Omega_r r^2} \right) - 2 \sinh(\mu)^2 \right) + \frac{1 - \alpha}{2} + \frac{\alpha}{2\gamma} \quad (12)$$

where  $\Omega_r$  is the real part of the dimensionless  $\Omega$  and the dimensionless amplitude ratio of bottom to surface

$$\alpha = \frac{a_s^2}{a_b^2} = \cosh^2 \mu \left( 1 - \frac{\mu \tanh \mu}{\Omega^2} \right) \quad (13)$$

with  $a_s(t) = a_{s0} e^{\omega_i t}$ . The energy in dimensionless form is then written as

$$\varepsilon = \frac{E}{E_0} = \frac{1}{2} e^{2\Omega_i \tau} D_d \quad (14)$$

with  $E_0 = 1/2 \rho g a_s^2$  and  $\tau = t \sqrt{\frac{g}{h}}$ .

The energy in the carpet for one period of time is then

$$E_c = \frac{1}{2} \rho g a_{s0}^2 \varepsilon A_c \quad (15)$$

where  $A_c$  represents the carpet area.

## EXPERIMENTAL DETAILS

### Wave tank and wave maker

The experiments were carried out in a 30 m long, 0.45 m wide, and 2.4 m high wave tank. A schematic diagram of the wave tank is shown in figure 3. The inside surface of the tank consists of a set of large flat panels which are in turn supported by a structure consisting of steel beams. All of the floor panels and the wall panels at the two ends of the tank are made of stainless steel plates, while the panels on the long sidewalls of the tank are made of clear plastic. A flap-type wave-maker is located at one of the far ends of the wave tank. The wave maker is powered by a motor. The wave board is hinged at the bottom of the wave tank and is connected through a shaft to the motor. The wave board spans through the entire width of the wave tank to prevent waves on the back side of the wave board. The wave maker creates waves to simulate several sea-states. The wave energy converter is installed at the bottom of the wave tank. Fig. 4 shows a photograph of the wave tank, the CWEC device, and the Power Take Off (PTO) system.

### Wave carpet

A schematic diagram of the carpet of wave energy converter is shown in Fig. 5. The CWEC has four major components: absorber carpet, connections, power take-of system (PTO), and mooring system. The absorber carpet passes the absorbed energy of the incident waves to the connections, which in turn transmit the energy to the hydraulic PTO units. The PTO units convert the translational kinetic energy into mechanically usable energy. The mooring system connects the bottom of the PTO units to the bottom of the wave tank. Fig. 6 shows the solid model of the double acting pump along with a photograph.

## EXPERIMENTAL RESULTS AND DISCUSSION

A detailed set of experiments was conducted to assess the performance of the Wave Carpet under the load of highly nonlinear surface waves. The performance

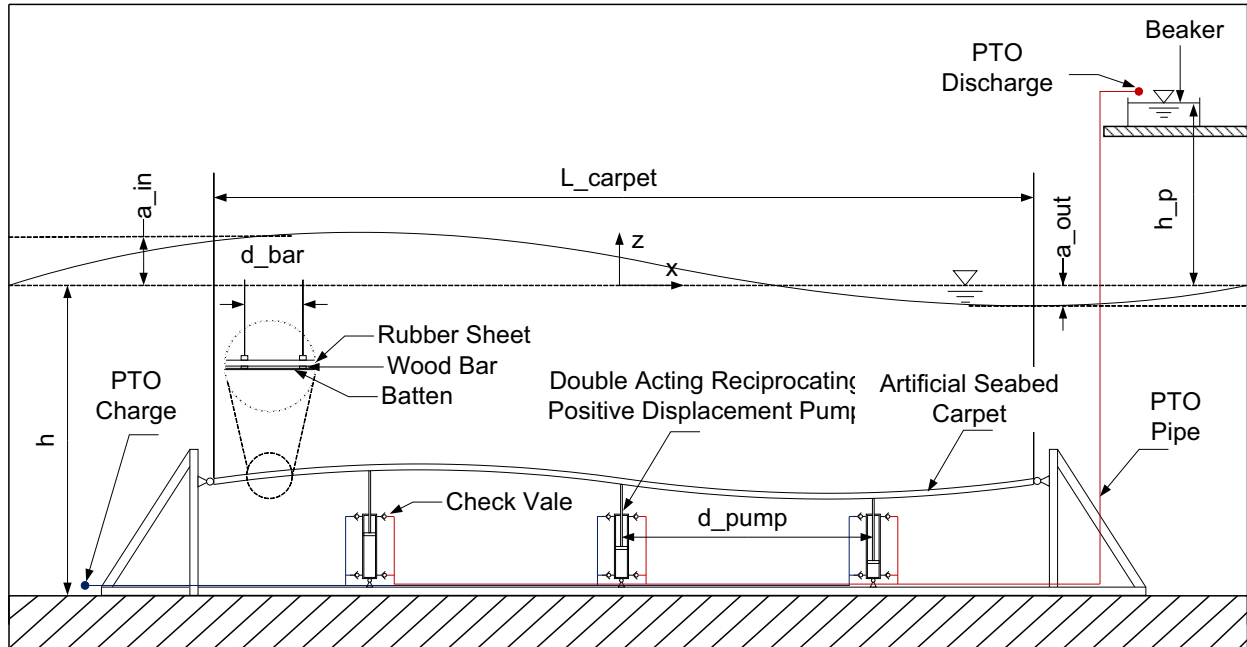


**Figure 3:** Schematic diagram of the experimental setup showing part of wave tank, wave carpet, and the PTO. The artificial seabed carpet is displaced by the overpassing waves incident from the left side. The shafts of the double acting reciprocating positive displacement pumps are connected to the carpet and are distributed equally. Through the displacement of the piston, water is pumped from the PTO charge to the PTO discharge. The water flow rate at the discharge with a height of  $h_p$  and the wave amplitudes of  $a_{in}$  and  $a_{out}$  are measured.



**Figure 4:** A photograph of the wave tank and the wave carpet along with the PTO.

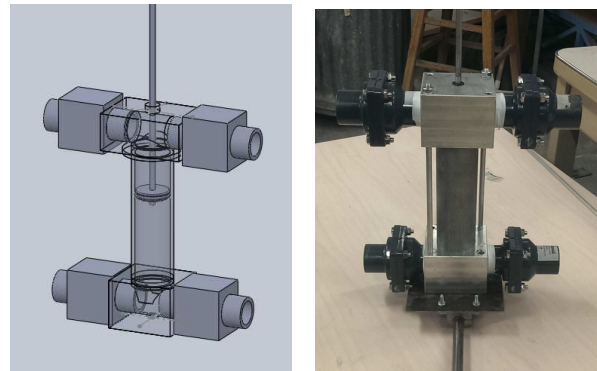


**Figure 6:** (Left) A solid model and (right) a photograph of the double acting pump used throughout the current experiments.

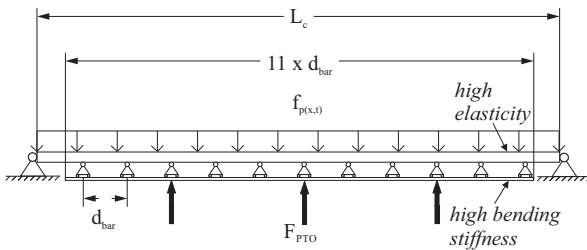


**Figure 5:** Mechanical model of the wave carpet.

criteria used to evaluate the functionality of the operating system are the total and absorption efficiencies of the carpet. The experiments were carried out for a range of parameters to compare the performance of the device for different sea states with different operation settings. The wave frequency and the wave height were chosen as the wave parameters, resulting in a variety of incident wave energy and the ratio of the carpet length to the wavelength.

In order to investigate the effects of the carpet properties on the absorption and conversion efficiencies of the overall system, two different carpet settings were tested. The stiffness of the device was varied using two fiberglass sets b1 and b2. The stiffness of the composite carpet is determined by the fiberglass bars. The flexural rigidity or stiffness represents the spring coefficient  $k^*$ .

On the mechanical system level, the pump height represents the damping coefficient  $b^*$ , as the bore of the PTO units were held constant. Three pump heights of  $h_p = 1.82\text{ m}$ ,  $3.69\text{ m}$ , and  $5.5\text{ m}$  were used throughout the current study. The goal of the experimental investigations are the conversion efficiency of the system for different system parameters  $b^*$  and  $k^*$ .

The water level is held constant at  $h = 0.74\text{ m}$ . The wave amplitude  $a_{in}$  and  $a_{out}$  were measured using an imaging technique. Due to an influential partial standing wave, the true standing wave was extracted using the method described by Goda and Suzuki. Fluorescent dye was illuminated using back lighting to highlight the surface of the water against a dark background. The water flow rate was measured manually by stopping the filling time of a standardized volume of  $3000\text{ ml}$  at the height of  $h_p$  above the mean water level.

The total efficiency of the PTO system is calculated as

$$\eta_{total} = \frac{P_{PTO}}{P_{wave}} \quad (16)$$

with

$$P_{PTO} = P_{pot} + P_{kin} = \rho \dot{V} g h_p + \frac{1}{2} \rho \dot{V} v_{free}^2 \quad (17)$$

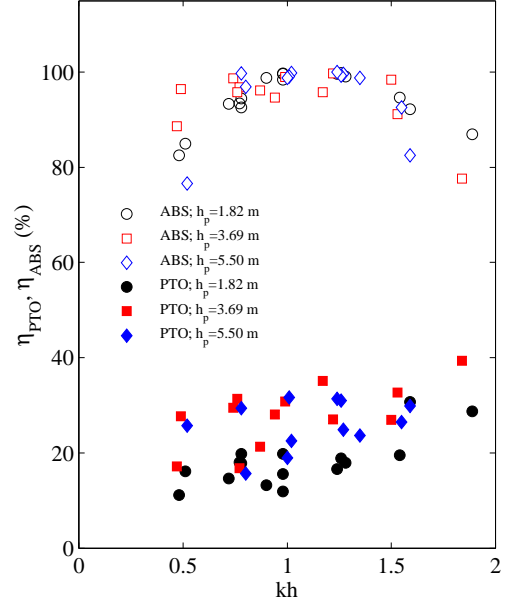
where

$$v_{free} = \frac{\dot{V}}{A_{out}} \quad (18)$$

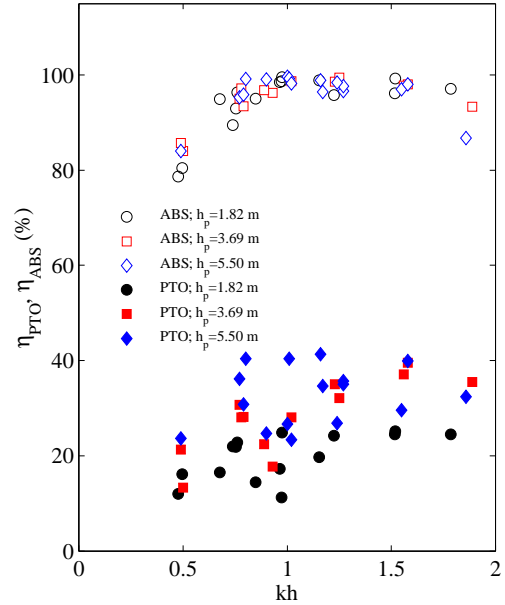
The cross sectional area of the free jet at the PTO discharge is  $A_{out} = 1.2610^{-4}\text{ m}^2$ . The kinetic power of the free jet for the given experimental parameters is in the order of  $10^{-10}\text{ W}$  and is therefore negligible. The wave power converted by the prototype is the power of the wave entering the control volume. The wave power is then calculated as

$$P_{wave} = \frac{1}{2} \rho g C_g a_{in}^2 W \quad (19)$$

with a wave tank width of  $W = 0.45\text{ m}$ , wave amplitude of  $a_{in}$  just before the wave reaches the setup, the gravitational acceleration of  $g$ , water density of  $\rho = 999\text{ kg/m}^3$  at the room temperature. The group velocity of the wave is



(a)



(b)

**Figure 7:** Measured PTO and absorption efficiencies for three different pump heights  $h_p$  versus shallowness for the stiffness value of (a) b1 and (b) b2.

$$C_g = \frac{g \tanh(kh) - gkh(\tanh^2(kh) - 1)}{2\sqrt{gk \tanh(kh)}} \quad (20)$$

Using equations 17 and 19, the average total efficiency

is calculated as

$$\eta_{total} = \frac{4\dot{V}h_p\sqrt{gk\tanh(kh)}}{gWa_{in}^2(\tanh(kh) - kh(\tanh^2(kh) - 1))}. \quad (21)$$

The total efficiency reflects the ability of the device to convert the energy of the incident waves into hydraulically usable energy and thus its performance. In addition, the absorption efficiency reflects the ability of the device to dissipate the energy of the incident waves and is calculated as

$$\eta_{ABS} = \frac{E_{in} - E_{out}}{E_{in}} = \frac{a_{in}^2 - a_{out}^2}{a_{in}^2}. \quad (22)$$

The simulated range of wave parameters are summarized in the dimensionless values of shallowness  $kh$ , steepness  $ka$  and  $a/h$ . To satisfy the linear theory, shallowness  $kh$  and steepness  $a/h$  should be less than 0.3. Fig. 7 shows  $\eta_{PTO}$  and  $\eta_{ABS}$  for different wave shallowness values for the six combinations of possible device parameters. The efficiency of the device for the range of wave parameters has a stronger correlation with the variation of  $b^*$  than  $k^*$ . As shown in Fig. 7, the efficiency of  $b^*(h_p = 5.5)$  is higher than  $b^*(h_p = 3.69)$  and  $b^*(h_p = 1.82)$ . A peak efficiency of 42.3% was obtained for  $b2$  and  $h_p = 5.5m$ , representing a combination of the highest stiffness and damping. A slight upward trend of the efficiency for higher shallowness values was also obtained. For the two lower values of  $b^*$ , the efficiencies with  $k^*(b1)$  and  $k^*(b2)$  are in the same order, whereas for the highest  $b^*(h5)$ , higher efficiencies were achieved with higher stiffness  $k^*(b2)$ . Therefore, for a higher stiffness value, a higher damping leads to higher efficiencies. As the shallowness is varied, no specific correlation between absorption efficiency and the system parameters  $b^*$  and  $k^*$  is noticed and the values range from 85 to 99%. The peak value of 99.609% is again reached for  $b2$  and  $h_p = 5.5m$ .

Figs. 8 and 9 show  $\eta_{PTO}$  and  $\eta_{ABS}$  for different wave steepness values,  $ka$  and relative wave heights,  $a/h$ . The figures show that for an increase in damping coefficient, the wave steepness has a stronger effect on the efficiency of the system. As the steepness is varied, no specific correlation between absorption efficiency and the system parameters  $b^*$  and  $k^*$  is noticed.

Furthermore, Fig. 10 shows the displacement of the three units with time. The figure shows that the maximum displacement occurs at the second pump while the first pump displacement is still larger than the displacement of the third pump. This can be explained due to

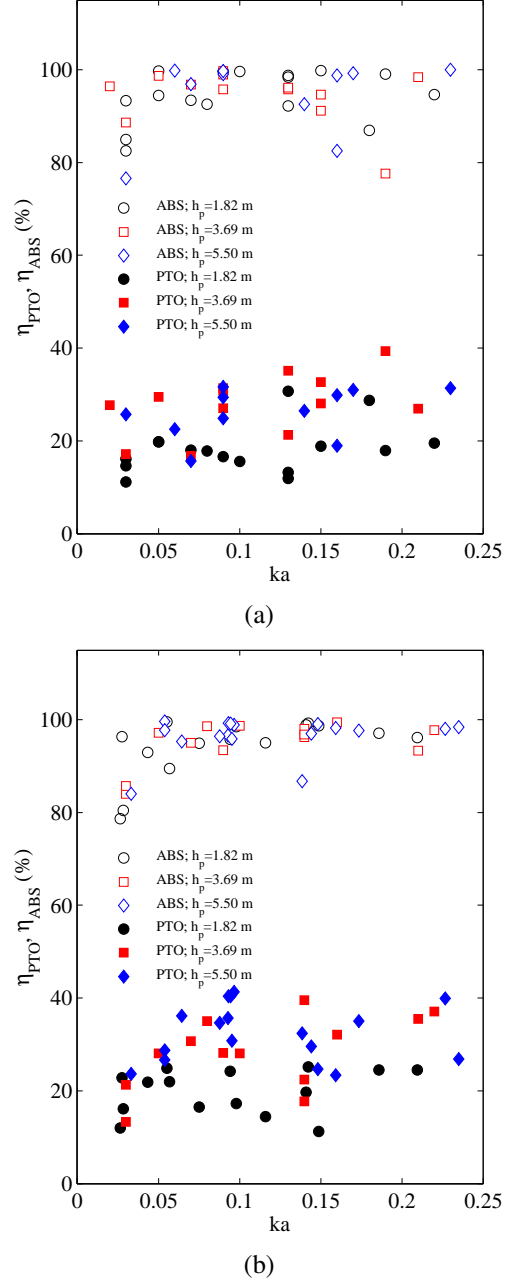
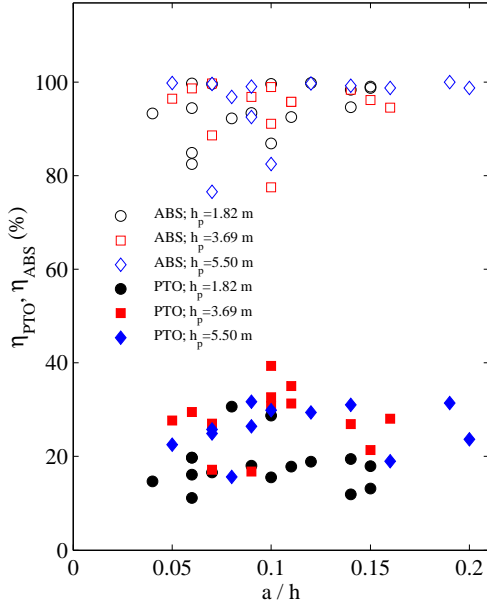
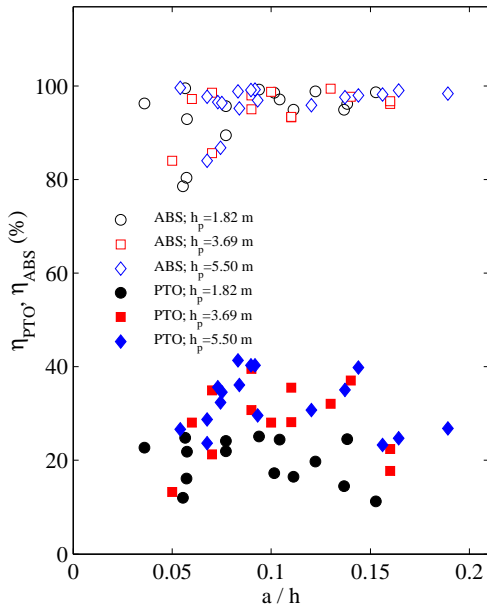


**Figure 8:** Measured PTO and absorption efficiencies for three different pump heights  $h_p$  versus wave steepness for the stiffness value of (a)  $b1$  and (b)  $b2$ .

the fact that the second pump has the maximum distance to the side mounting points of the absorber carpet while being exposed to the highest load on the carpet. The first pump is accelerated by the carpet area that first interacts with the incoming wave and thus has a lower fraction of the wave period time to interact and absorb the wave energy. The last pump has the least amount of displacement due to the fact that at this propagation



(a)



(b)

**Figure 9:** Measured PTO and absorption efficiencies for three different pump heights  $h_p$  versus relative wave height for the stiffness value of (a) b1 and (b) b2.

distance, most of the wave energy is already absorbed and converted by the two previous pumps and their designated absorption area.

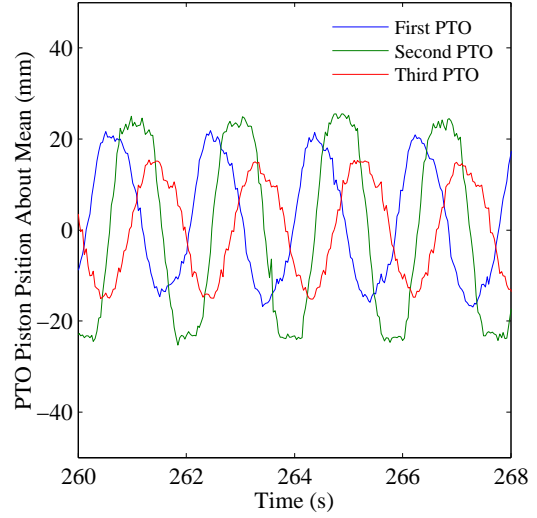


**Figure 10:** Displacement of the three individual PTO units over time.

## CONCLUSIONS

The main objective of current study was analytical modeling and experimental assessment of the Wave Carpet under a broad range of system parameters. An analytical solution for the motion of the pressure differential wave energy converter and the system's ability to extract wave energy was presented. The process of transferring and optimizing the initial mechanical concept to a first working and optimized prototype was also set forth. The main components of the system are a synthetic seabed carpet, a direct physical connection, a hydraulic Power Take Off system and a mooring component. The energy stored in the overtopping waves is damped out by the absorber carpet and converted into hydraulic energy using double acting linear reciprocating pumps that are directly connected to the absorber carpet. The engineering challenge of an absorber carpet material with anisotropic material properties was addressed using a composite material that has the ability of a changeable stiffness. The results of the experiments are a detailed quantification of the efficiency of the developed PTO units. The functionality of the prototype was successfully tested. A peak experimental PTO and absorption efficiency of **42.3%** and **99.33%** was achieved, respectfully.

## ACKNOWLEDGEMENT

The financial support from the American Bureau of Shipping is gratefully acknowledged. The authors would like to thank the Machine Shop in the Depart-

ment of Mechanical Engineering, UC Berkeley for their continuous and enthusiastic support. Authors would like to acknowledge Ryan Feng, Ricardo Maldonado, Thomas Boerner and Reza Ghorbani for their help during fabrication and conducting the experiments.

## REFERENCES

- Alam, M.-R., “Nonlinear analysis of an actuated seafloor-mounted carpet for a high-performance wave energy extraction.” Proceedings of the Royal Society A: Mathematical, Physical and Engineering Sciences. doi:10.1098/rspa.2012.0193, 2012a.
- Alam, M.-R. “A flexible seafloor carpet for high-performance wave energy extraction.” Proceedings of the ASME 2012 31st International Conference on Ocean, Offshore and Arctic Engineering OMAE2012 July 1-6, 2012, Rio de Janeiro, Brazil (OMAE2012-84034), 2012b.
- Creel, L. “Ripple effects: Population and coastal regions.” Population Reference Bureau 12.4 (2003): 500.
- Elgar, Steve and Raubenheimer, Britt. “Wave dissipation by muddy seafloors.” Geophysical Research Letters 35.7 (2008): L07611.
- Mork, G., Pontes, M.T., Barstow, M.T., and Kabuth, A. “Assessing the global wave energy potential.” 29 th International conference on Ocean, Offshore Mechanics and Arctic Engineering. Shanghai, China, 2010.
- Gade, H G. “Effects of a non-rigid, impermeable bottom on plane surface waves in shallow water.” Journal of Marine Research 16: 61–82, 1958.
- Ibrahima, H., Perronb, J., Ilincaa, A. “Energy storage systems: Characteristics and comparisons.” Renewable and Sustainable Energy Reviews 12: 1221–1250, 2008.
- Holland, K Todd, Vinzon, Susana B, and Calliari, Lauro J. “A field study of coastal dynamics on a muddy coast offshore of Cassino beach, Brazil.” Continental Shelf Research 29.3 (2009): 503–514.
- Lehmann, M., Elandt, R., Pham, H., Ghorbani, R., Shakeri, M., and Alam, M.-R. “An artificial seabed carpet for multidirectional and broadband wave energy extraction : Theory and Experiment.” Proc. 10th Europ. Wave & Tid. Ener. Conf., EWTEC2013, 2-5 Sept. 2013, Aalborg, Denmark. 2013.
- Macpherson, H., and Kurup, P. G. “Wave damping at the Kerala mudbanks, southwest India.” Indian Journal of Marine Science 10: (1981) 154–160.
- U.S. Department of Energy, “Energy demands on water resources.”, Technical Report, U.S. Department of Energy, 2006.
- Pahl, G. Engineering design: A systematic approach. Berlin Heidelberg: Springer-Verlag, 2007.
- Payne, G. Guidance for the experimental tank testing of wave energy converters. The University of Edinburgh, 2008.
- Sheremet, A. and Stone, G.W. “Observations of nearshore wave dissipation over muddy sea beds.” Journal of Geophysical Research 108.C11 (2003): 1–11.
- Silvester, R. Coastal Engineering. Elsevier, 1974.